Medicine®

OPEN

Diagnostic performance of dual-energy computed tomography for HCC after transarterial chemoembolization

Utility of virtual unenhanced and low keV virtual monochromatic images

Joonho Hur, MD[a,b], Eun Sun Lee, MD, PhD[b,c],* , Hyun Jeong Park, MD, PhD[b,c], Woosun Choi, MD, PhD[b,c], Sung Bin Park, MD, PhD[b,c]

Abstract

The purpose of this study is to evaluate the usefulness of virtual unenhanced (VUE) and low keV virtual monochromatic images (VMI) for diagnosing viable hepatocellular carcinomas (HCC) after transarterial chemoembolization (TACE).

This retrospective study included 53 patients with suspected viable HCC after TACE who underwent multiphasic liver computed tomography including true unenhanced (TUE) phase and conventional (CV) enhanced phases on a dual-energy scanner. VUE images, 40 keV and 55 keV VMIs of enhanced phases were reconstructed using dual-energy computed tomography data. For every patient, six combination image sets (TUE-CV; TUE-55; TUE-40; VUE-CV; VUE-55; VUE-40) were evaluated by two readers and compared with the reference standard.

There was no statistically significant difference ($P > .05$) in sensitivity or specificity among all image combinations. In most combinations, interobserver agreements were almost perfect. The diagnostic odds ratio showed a higher trend in combinations with conventional images.

Currently, with regards to diagnostic performance, liver computed tomography including TUE and CV enhanced phases is recommended for tumor surveillance after TACE because VUE and VMIs do not have a distinct advantage compared to conventional images.

Abbreviations: CT = computed tomography, CV = conventional, DE = dual-energy, HCC = hepatocellular carcinoma, MRI = magnetic resonance imaging, PVP = portal venous phase, TACE = transarterial chemoembolization, TUE = true unenhanced, VMI = virtual monochromatic image, VUE = virtual unenhanced.

Keywords: dual-energy computed tomography, hepatocellular carcinoma, transarterial chemoembolization, virtual monochromatic image, virtual unenhanced image

1. Introduction

Hepatocellular carcinoma (HCC) is the fifth most common cancer and the second most common cause of cancer deaths worldwide.[1] Recently, the incidence of HCC has been increasing,[2] despite remarkable improvements for the treatment of viral hepatitis, such as vaccination against the hepatitis B virus or several effective anti-viral drugs, since the 1980's.[3–5]

Transarterial chemoembolization (TACE) is a commonly used treatment option for intermediate- or advanced-stage HCCs.[1] Treatment-response monitoring and surveillance of new HCCs in patients who underwent TACE are routinely performed using conventional imaging, such as contrast enhanced computed tomography (CT) or magnetic resonance imaging (MRI). Although high-quality MRI is the best imaging modality for patients undergoing repeated TACE owing to excellent soft tissue contrast and irrelevancy to ethiodized oil deposition, contrast enhanced CT is the most widespread imaging tool because of its cost-effectiveness and rapid acquisition. However, detecting viable HCC using CT after TACE can be challenging owing to altered hemodynamics of tumor and beam-hardening artifacts caused by hyperattenuating ethiodized oil depositions.[6–9] Thus, conventional CT scans may have a decreased diagnostic ability, particularly for small

HCC showing atypical enhancement pattern around the previously embolized lesion.[10]

With the advancement of CT technology, dual-energy (DE) CT has the capability to perform material decomposition that can reconstruct virtual monochromatic images (VMI) or virtual unenhanced (VUE) images. Recently, several studies reported increased detection of HCC, including small-sized HCC, using low KeV imaging on DE-CT scan.[11–13] Furthermore, as worldwide interest in radiation exposure has increased, there is a concern regarding the cumulative radiation dose during life-long HCC surveillance in chronic liver disease patients. Therefore, there is growing interest in whether VUE could replace true unenhanced (TUE) images to lower the radiation dose by approximately 2/3 in a 3-phase scan.[14] However, there are concerns regarding image quality, increase in noise, and unverified diagnostic accuracy.[12,13,15]

Therefore, this study aimed to evaluate the efficacy of VUEs and VMIs for the diagnosis of viable HCCs after TACE.

2. Materials and Methods

2.1. Patients

This study was approved by the Institutional Review Board (IRB No. 2011-012-19341) of our institution. Owing to the retrospective nature of this study, written informed consent was waived. From March 2020 to September 2020, 103 consecutive patients with suspected viable hepatocellular carcinoma by clinician after conventional TACE who underwent multiphasic liver CT imaging on a DE-CT scanner (IQon spectral CT; Philips Healthcare, Best, Netherlands) were enrolled. Liver MRI or angiography within 6 months of CT was used as a reference standard. Among the 103 patients, 29 patients without history of conventional TACE (consist of receiving a mixture of doxorubicin (Adriamycin; Ildong Pharmaceutical Co., Ltd, Seoul, Korea) emulsified with ethiodized oil (Lipiodol; Guerbet, Paris, France), followed by embolization with particles) at our institution, 17 patients without reference standard within 6 months, and four patients with diffuse infiltrative HCC were excluded. Finally, a total of 53 patients were included in this study.

2.2. Image acquisition and reconstruction

All multiphasic liver CT scans were obtained in one dual-energy spectral CT (IQon spectral CT; Philips Healthcare) machine

and consisted of TUE phase, arterial phase (AP), portal venous phase (PVP), and delayed phase (DP) images in all patients. TUE phase was obtained using 100 kVp of tube voltage and tube current was automatically modulated with an average of 130 mAs (maximum 280 mAs). Enhanced phases were obtained using 120 kVp of tube voltage and tube current was automatically modulated with an average of 82 mAs (maximum 250 mAs). The iodinated contrast medium (Pamiray 370; Dongkuk Pharm., Seoul, Korea) was intravenously injected at a dose of 1.5 mL/kg of body weight at a rate of 3.5 mL per second. Bolus-tracking technique was used for enhanced phase scan; the AP scan was started 25 second after the attenuation of the abdominal aorta reached 150 HU (80 seconds for PVP; and 3 minutes for DP). We used iterative reconstruction (iDose level 4; Philips Healthcare) for all conventional images. The other parameters were as follows: detector collimation, 64.0 × 6.25; pitch, 0.921; slice thickness, 3 mm; and reconstruction interval, 3 mm.

Virtual unenhanced images (VUE) were reconstructed using PVP images from DE-CT data for comparison with the true unenhanced (TUE) images (Fig. 1). In addition, 40 keV (the lowest keV that can be reconstructed) and 55 keV (as median) VMIs of every enhanced phase were reconstructed, because the 70 keV VMI is equivalent to that of conventional (CV) images for a body in dual-layer DE-CT.[16] All image data were processed using IntelliSpace Portal software 11.1 (Philips Healthcare). Using these images, six combination image sets (TUE-CV; TUE-55; TUE-40; VUE-CV; VUE-55; VUE-40) were created for every patient (Fig. 1). Finally, 318 image combination sets of 53 patients were the subject of image analysis.

2.3. Image analysis

Two board-certified abdominal radiologists (E.S.L. and H.J.P., with 15 years of clinical experience each), who were blinded to the clinical and technical details, independently evaluated all image combination sets (n = 318) for the presence of LR-TR viable lesion according to the LI-RADS treatment response algorithm in each patient; the image sets were randomly sorted. For the comparison with the reference standard, the presence of viable tumors and, if any, the location of the most concerning lesion were assessed. The time interval between the CT scan and reference standard was limited to 6 months. The reference standard for HCC was as follows: (1) LR-TR viable lesion on magnetic resonance imaging; (2) hypervascular tumor on digital
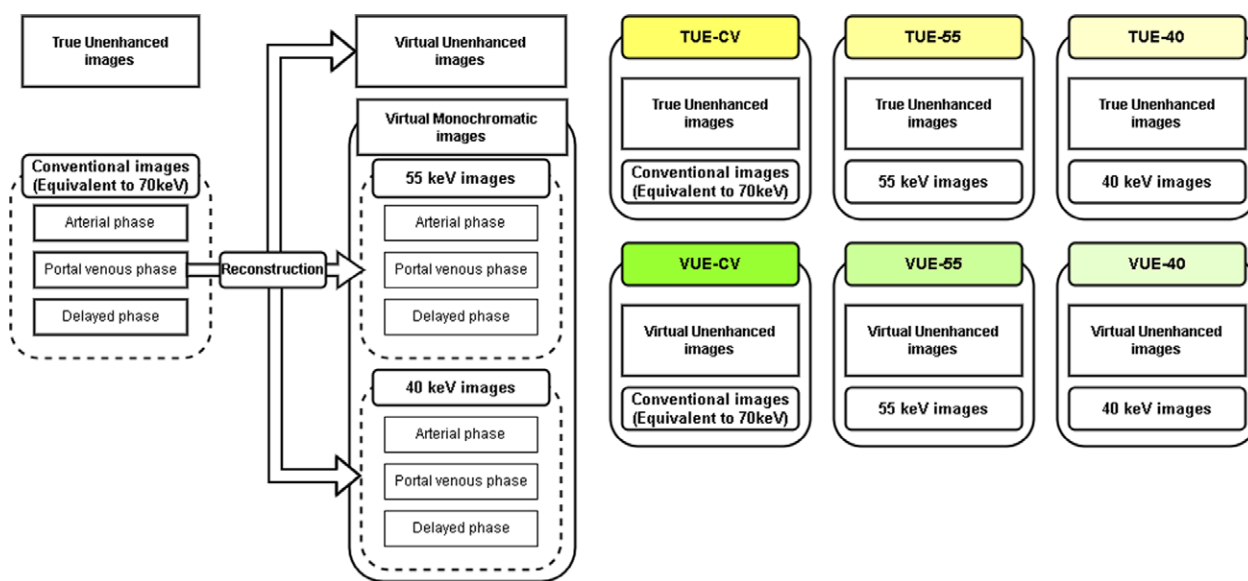

Figure 1. Flow diagram of image reconstruction and combination image sets.

subtraction angiography (DSA) and focal compact ethiodized oil uptake on sequential CT.[17,18] Finally, one board-certified radiologist (J.H., with 9 years of clinical experience) evaluated the diagnostic performance compared with the reference standard.

2.4. Statistical analysis

Statistical analysis was performed using SPSS statistics version 26 (IBM Corp., Armonk, NY, USA). Sensitivity, specificity, positive predictive value, and negative predictive value of the imaging parameters in CT were calculated. Categorical variables were compared using chi-squared or Fisher exact tests as appropriate. Interobserver agreement between the 2 radiologists was calculated using Cohen kappa (κ) coefficient and all κ values were interpreted according to the following: poor, a κ value of 0.19 or lower; fair, a κ value of 0.20–0.39; moderate, a κ value of 0.40–0.59; substantial, a κ value of 0.60–0.79; and almost perfect, a κ value of 0.80–1.00. A *P*-value <.05 was considered statistically significant.

3. Results

Patient demographics, etiology, time interval from TACE, type of reference imaging used, time interval between DE-CT and reference imaging, and number of HCCs in each patient are summarized in Table 1. Only 1 patient had 5 days of interval from previous TACE, but the other patients had more than 3 weeks. All patients showed retained ethiodized oil deposition in the liver from previous TACE. There were 29 patients with viable HCC on reference standard, 8 of which had multiple lesions. The size of viable lesions on reference standard was varied from 4 to 21 mm. Assessments of each combination in 2 readers are summarized in Table 2. Among each combination of images, there was no statistically significant difference (*P* > .05) in sensitivity or specificity, but combination with 40 keV sets showed the lowest value in terms of sensitivity and specificity in both readers (Table 3). Accuracy of image sets tended to be

Table 1
Patient characteristics.

Age	Yrs
Median	72
Range	54–91
Gender	No. of patients (%)
Male	39 (73.6)
Female	14 (26.4)
Etiology of liver disease	No. of patients (%)
Hepatitis B	25 (47.2)
Hepatitis C	12 (22.6)
Hepatitis B + C	1 (1.9)
Alcohol	12 (22.6)
Nonalcoholic steatohepatitis	2 (3.8)
Unknown	1 (1.9)
Interval from previous TACE	Days
Median	92
Range	5–2923
Type of reference standard	No. of patients (%)
Magnetic resonance imaging	32 (60.4)
Angiography and computed tomography	21 (39.6)
Reference interval	
Median	91
Range	0–180
No. of HCC lesions	No. of patients (%)
Negative	24 (45.3)
Single	21 (39.6)
Multiple	8 (15.1)

HCC = hepatocellular carcinoma, TACE = transarterial chemoembolization.

Table 2
Assessments of each combination in two readers.

		Reader 1			Reader 2	
		Standard reference			**Standard reference**	
		Viable (n = 29)	**Nonviable (n = 24)**		**Viable (n = 29)**	**Nonviable (n = 24)**
TUE-CV	(+)	13	1	(+)	13	5
	(−)	16	23	(−)	16	19
TUE-55	(+)	12	5	(+)	12	5
	(−)	17	19	(−)	17	19
TUE-40	(+)	11	5	(+)	11	4
	(−)	18	19	(−)	18	20
VUE-CV	(+)	12	1	(+)	12	1
	(−)	17	23	(−)	17	23
VUE-55	(+)	11	2	(+)	12	1
	(−)	18	22	(−)	17	23
VUE-40	(+)	10	6	(+)	10	3
	(−)	19	18	(−)	19	21

CV = conventional, TUE = true unenhanced, VUE = virtual unenhanced.

higher in combinations with conventional images (i.e., equivalent to 70 keV). Interobserver agreements were almost perfect in TUE-CV, TUE-55, TUE-40, VUE-55, and VUE-40 sets and the highest agreement between 2 readers was 0.95 in TUE-CV (Table 3). VUE-CV image set showed substantial agreement. All *P* values of κ were less than .001 and, thus, statistically significant.

The diagnostic odds ratios (DORs) are shown in Table 4. In reader 1, only the TUE-CV set showed a statistically significant DOR of 18.69. In reader 2, TUE-CV, TUE-55, VUE-CV, and VUE-55 displayed statistically significant DORs of 16.24, 6.72, 16.24, and 16.24, respectively. There may be a higher trend in combinations with conventional images but no trend in combinations between TUE and VUE were observed.

4. Discussion and conclusions

In this retrospective study, we directly compared VUE and VMIs which is clinically applicable with conventional images using various combinations of image sets. Also, this is the first study evaluated both VUE and VMI in the clinical image using DE-CT image, after conventional TACE that can limit diagnostic accuracy, at our knowledge. It has been reported that low keV VMI shows improved conspicuity because of more evident iodine contrast at a close photon energy to the k-edge of iodine (33.2 keV) not only for the lesion in the liver parenchyma but also for in the evaluation of portal vein or bile duct tumor thrombus.[13,16,19–21] VMI can reduce beam-hardening artifacts at a relatively high keV level, such as 80 or 100 keV. In contrast, the beam-hardening artifact increases at a low keV VMI setting.[22] Since the conventional CT currently used is equivalent to approximately 70 keV, an increase in conspicuity and a decrease in beam-hardening artifact cannot be achieved in conjunction. More artifacts, such as beam-hardening or blooming of low keV VMI, may occur because of ethiodized oil deposition, particularly in CT performed after TACE (Fig. 2). In addition, an increase in noise with decreasing keV can affect the results, but clinically applicable imaging, features, such as vendor-specific automatic noise reduction, may reduce some of these effects.[23]

Unlike most previous studies assessing the initial diagnosis of HCC,[12,13,24] we compared VUE and TUE images in patients with HCC after conventional TACE. It has been reported that although soft tissue lesions, such as liver, spleen, fat, or vessels, show similar CT numbers between VUE, and TUE, there is a

Table 3

Comparison of CT image combinations and interobserver agreement.

	Reader 1					Reader 2					
	Sensitivity	Specificity	PPV	NPV	Accuracy	Sensitivity	Specificity	PPV	NPV	Accuracy	κ value
TUE-CV	0.45	0.96	0.93	0.59	0.68	0.41	0.96	0.92	0.58	0.66	0.95
TUE-55	0.41	0.79	0.71	0.53	0.58	0.38	0.92	0.85	0.55	0.62	0.82
TUE-40	0.38	0.79	0.69	0.51	0.57	0.34	0.75	0.63	0.49	0.53	0.91
VUE-CV	0.45	0.79	0.72	0.54	0.60	0.41	0.96	0.92	0.58	0.66	0.77
VUE-55	0.41	0.79	0.71	0.53	0.58	0.41	0.96	0.92	0.58	0.66	0.82
VUE-40	0.38	0.83	0.73	0.53	0.58	0.34	0.88	0.77	0.53	0.58	0.90

CT = computed tomography, CV = conventional, NPV = negative predictive value, PPV = positive predictive value, TUE = true unenhanced, VUE = virtual unenhanced.

Table 4

Diagnostic odds ratio and relative risk.

	Reader 1				Reader 2			
	Odds ratio	95% CI			Odds ratio	95% CI		
	Relative risk	Lower	Upper	P value	Relative risk	Lower	Upper	P value
TUE-CV	18.69	2.22	157.52	.001*	16.24	1.92	137.19	.002*
	2.26	1.51	3.39		2.17	1.47	3.22	
TUE-55	2.68	0.78	9.19	.111	6.72	1.32	34.32	.013*
	1.49	0.94	2.37		1.88	1.24	2.84	
TUE-40	2.32	0.67	8.01	.177	1.58	0.48	5.24	.454
	1.41	0.89	2.26		1.22	0.74	1.99	
VUE-CV	3.09	0.90	10.53	.066	16.24	1.92	137.19	.002*
	1.58	1.00	2.50		2.17	1.47	3.22	
VUE-55	2.68	0.78	9.19	.111	16.24	1.92	137.19	.002*
	1.49	0.94	2.37		2.17	1.47	3.22	
VUE-40	3.06	0.82	11.32	.087	3.68	0.88	15.42	.064
	1.55	0.98	2.44		1.62	1.04	2.52	

CI = confidence interval, CV = conventional, TUE = true unenhanced, VUE = virtual unenhanced.
*Statistically significant.
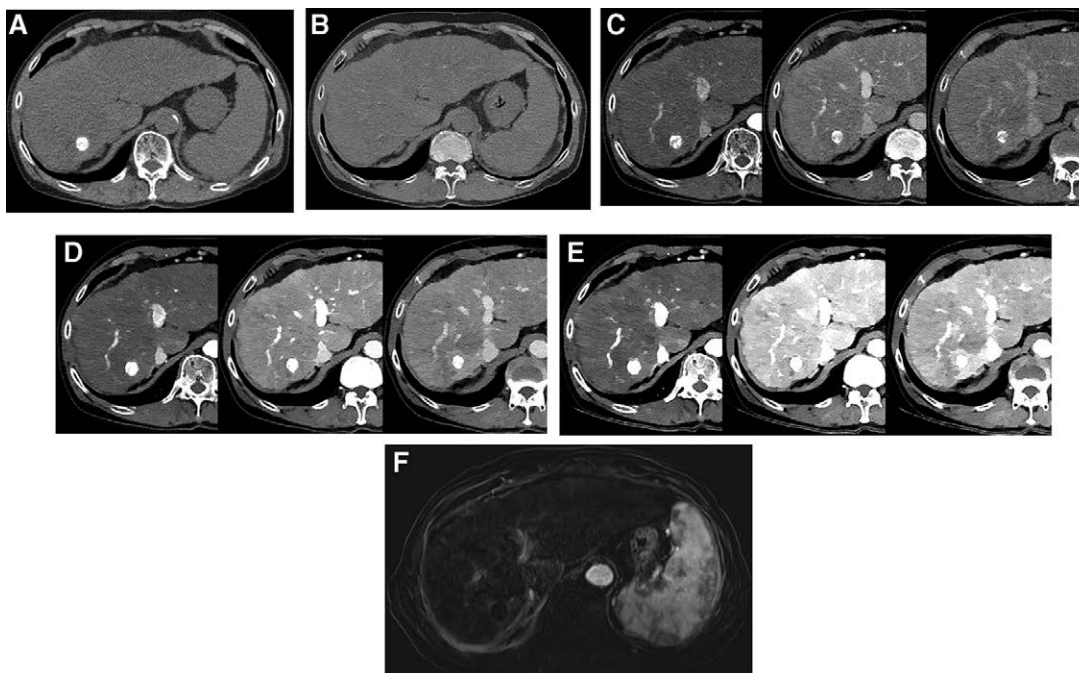
Figure 2. A 51-year-old male who underwent transarterial chemoembolization for hepatocellular carcinoma with underlying alcoholic liver cirrhosis 106 days prior. True unenhanced (TUE) image (A) shows dense ethiodized oil uptake in segment six of the liver. However, virtual unenhanced (VUE) image (B) shows excessive subtraction of ethiodized oil deposition. Arterial, portal venous, and delayed phases of conventional (CV) image (C), 55 keV (D) and 40 keV (E) virtual monochromatic images are displayed using the computed tomography window width and level of 400 and 100, respectively. As the keV is lowered, more blooming artifact of the dense ethiodized oil deposition is demonstrated. Subtracted T1-weighted arterial phase image (F) shows no viable tumor portion in magnetic resonance imaging after 114 days from computed tomography. Reader 1 assessed viable lesion in every combination set except TUE-CV, and reader 2 assessed viable lesion in every combination set except TUE-CV and VUE-CV. These viable assessments turned out to be false positive results.

decrease in CT number due to calcium subtraction for high-density lesions, such as bone in VUE images.[24,25] Similarly, there were several false positive cases that occurred owing to excessive subtraction of ethiodized oil deposition in VUE in our study (Fig. 2). In cases of excessive or inconsistent subtraction of ethiodized oil on VUE, it is worth noting that retained ethiodized oil on enhanced images may mimic enhancing viable HCCs and confuse radiologists. Although we failed to reveal a significant difference between VUE and TUE images in this study, excessive or inconsistent subtraction of ethiodized oil needs to be overcome to completely replace TUE with VUE, because the shape of ethiodized oil deposition is an important image finding in HCC after TACE.[26]

In addition, it has been reported that VUE images show inferior detection and characterization of liver lesions. Although they display similar CT numbers, because of the distortions, liver parenchyma and the degree of fat component may be misrepresented (Fig. 3).[14,24] Chronic liver disease occurs because of a variety of factors, and the proportion of parenchymal fat according to the underlying disease may differ significantly. These differences can also occur depending on BMI, but this was not included in our study because the medical records at the time of CT were not completely available. Further studies

are required, including the assessment of the effect of differences in background liver parenchyma on VUE images.

Herein, the diagnostic performance of CT for diagnosing HCC was inferior to the previous meta-analysis.[27] However, our study was based on CT after TACE, which is challenging because of altered hemodynamics and artifacts, and showed similar sensitivity and specificity to previous report for LR-TR viable lesion.[28] Although our results did not show satisfactory sensitivity, high specificity is important in order not to overlook subtle lesions in follow-up after TACE. Moreover, our results were meaningful owing to the relatively high DOR.

There were several limitations in our study. First, the sample size was small. This was because of the need for a time interval for the reference standard. In addition, although the time interval with the reference standard was limited to within 6 months, the results may be affected owing to new lesions during the time interval. Second, the study population had heterogenous histories of previous treatment. Although all patients had ethiodized oil deposition, the interval range from previous TACE was wide, and this may have affected the heterogeneity. Third, laboratory parameters, such as alpha-fetoprotein or PIVKA-II, were not included.

In conclusion, VMI does not yet have a distinct advantage for the patient with presence of many artifacts after TACE.
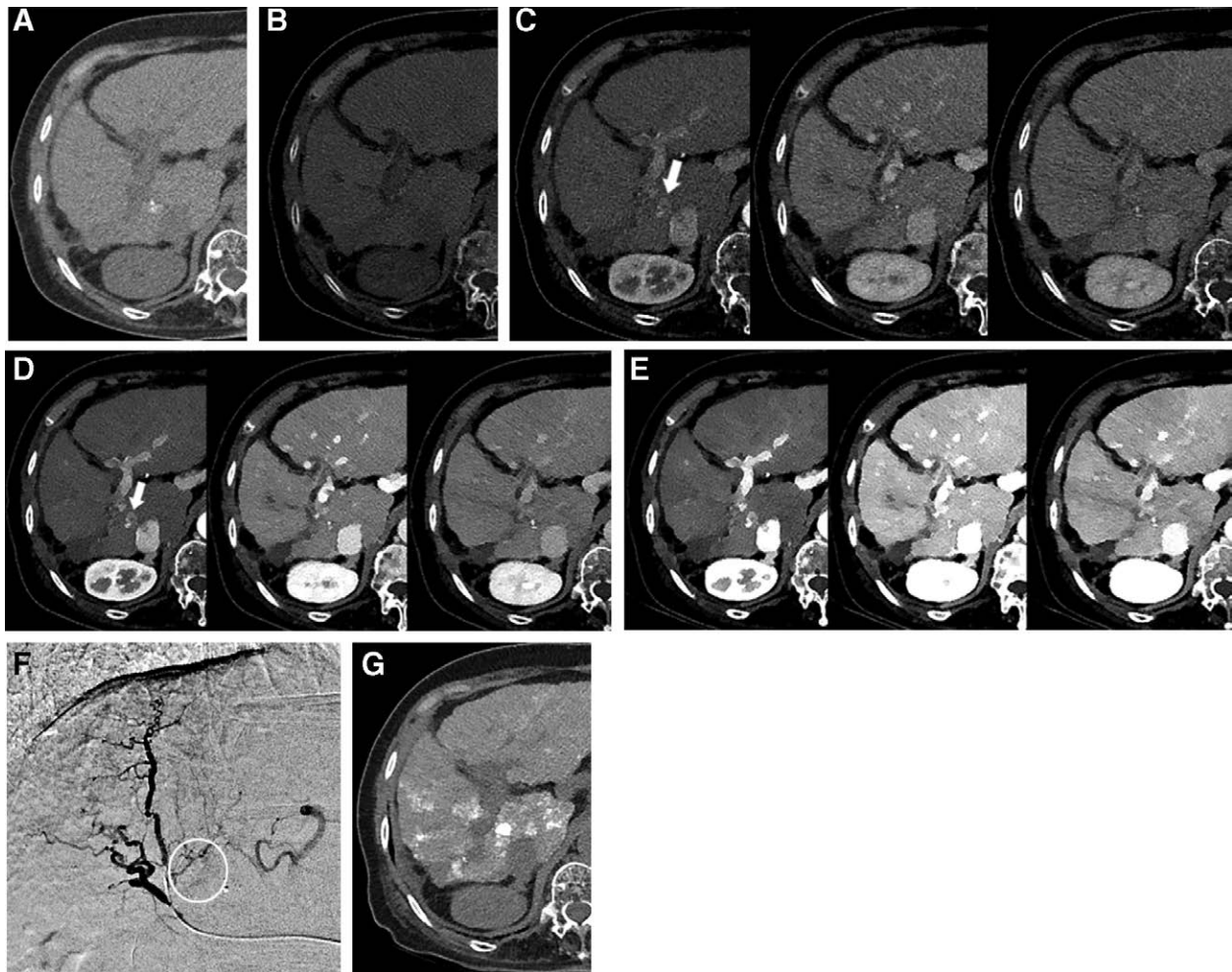
Figure 3. A 75-year-old male who underwent transarterial chemoembolization for hepatocellular carcinoma with underlying hepatitis B viral liver cirrhosis 575 days prior. Whereas true unenhanced (TUE) image (A) shows residual ethiodized oil uptake in segment one of the liver, virtual unenhanced (VUE) image (B) does not depict it well because of the over subtraction of ethiodized oil. Arterial, portal venous, and delayed phases of conventional (CV) image (C), 55 keV (D), and 40 keV (E) virtual monochromatic images are displayed using the computed tomography window width and level of 400 and 150, respectively. Both readers assessed viable lesions (arrow) in TUE-CV and TUE-55. However, they failed lesion detection in all VUE and TUE-40 combination sets. This patient underwent additional transarterial chemoembolization for viable tumor staining (white circle) demonstrated on the digital subtraction angiography (DSA) (F). Focal compact ethiodized oil uptake, which means viable tumor, is demonstrated on sequential CT (G).

In addition, although VUE image can lower the cumulative dose, its efficacy is not yet satisfactory. Therefore, it is thought that a palliative approach should be adopted, particularly for tumor surveillance. Further studies are required to determine imaging combinations with a lower cumulative radiation dose, better conspicuity for arterial enhancement, and fewer artifacts.

Acknowledgments

Author contributions

Conceptualization: Eun Sun Lee
Data curation: Joonho Hur, Woosun Choi
Formal analysis: Joonho Hur
Funding acquisition: Sung Bin Park
Investigation: Eun Sun Lee, Hyun Jeong Park
Methodology: Joonho Hur, Eun Sun Lee
Resources: Eun Sun Lee
Visualization: Joonho Hur
Writing – original draft: Joonho Hur, Eun Sun Lee
Writing – review & editing: Joonho Hur, Eun Sun Lee

References

[1] EASL Clinical Practice Guidelines. Management of hepatocellular carcinoma. J Hepatol. 2018;69:182–236.

[2] Llovet JM, Kelley RK, Villanueva A, et al. Hepatocellular carcinoma. Nat Rev Dis Primers. 2021;7:6.

[3] Dusheiko G, Main J, Thomas H, et al. Ribavirin treatment for patients with chronic hepatitis C: results of a placebo-controlled study. J Hepatol. 1996;25:591–8.

[4] Childs-Kean LM, Hand EO. Simeprevir and sofosbuvir for treatment of chronic hepatitis C infection. Clin Ther. 2015;37:243–67.

[5] Hoofnagle JH, Mullen KD, Jones DB, et al. Treatment of chronic non-A, non-B hepatitis with recombinant human alpha interferon. A preliminary report. N Engl J Med. 1986;315:1575–8.

[6] Jang KM, Choi D, Lim HK, et al. Depiction of viable tumor in hepatocellular carcinoma treated with transarterial chemoembolization: multiphasic helical CT with review of the previous serial CT images. Korean J Radiol. 2005;6:153–60.

[7] Kim HC, Kim AY, Han JK, et al. Hepatic arterial and portal venous phase helical CT in patients treated with transcatheter arterial chemoembolization for hepatocellular carcinoma: added value of unenhanced images. Radiology. 2002;225:773–80.

[8] Kim TK, Choi BI, Han JK, et al. Nontumorous arterioportal shunt mimicking hypervascular tumor in cirrhotic liver: two-phase spiral CT findings. Radiology. 1998;208:597–603.

[9] Silva AC, Morse BG, Hara AK, et al. Dual-energy (spectral) CT: applications in abdominal imaging. Radiographics. 2011;31:1031–46. discussion 10471050.

[10] Vande Lune P, Abdel Aal AK, Klimkowski S, et al. Hepatocellular carcinoma: diagnosis, treatment algorithms, and imaging appearance after transarterial chemoembolization. J Clin Transl Hepatol. 2018;6:175–88.

[11] Liu QY, He CD, Zhou Y, et al. Application of gemstone spectral imaging for efficacy evaluation in hepatocellular carcinoma after transarterial chemoembolization. World J Gastroenterol. 2016;22:3242–51.

[12] Lv P, Lin XZ, Chen K, et al. Spectral CT in patients with small HCC: investigation of image quality and diagnostic accuracy. Eur Radiol. 2012;22:2117–24.

[13] Yoo J, Lee JM, Yoon JH, et al. Comparison of low kVp CT and dual-energy CT for the evaluation of hypervascular hepatocellular carcinoma. Abdom Radiol (NY). 2021;46:3217–26.

[14] Ananthakrishnan L, Rajiah P, Ahn R, et al. Spectral detector CT-derived virtual non-contrast images: comparison of attenuation values with unenhanced CT. Abdom Radiol (NY). 2017;42:702–9.

[15] Li B, Pomerleau M, Gupta A, et al. Accuracy of dual-energy CT virtual unenhanced and material-specific images: a phantom study. AJR Am J Roentgenol. 2020;215:1146–54.

[16] Rassouli N, Etesami M, Dhanantwari A, et al. Detector-based spectral CT with a novel dual-layer technology: principles and applications. Insights Imag. 2017;8:589–98.

[17] Herber S, Biesterfeld S, Franz U, et al. Correlation of multislice CT and histomorphology in HCC following TACE: predictors of outcome. Cardiovasc Intervent Radiol. 2008;31:768–77.

[18] Langenbach MC, Vogl TJ, von den Driesch I, et al. Analysis of Lipiodol uptake in angiography and computed tomography for the diagnosis of malignant versus benign hepatocellular nodules in cirrhotic liver. Eur Radiol. 2019;29:6539–49.

[19] Nakamura Y, Higaki T, Honda Y, et al. Advanced CT techniques for assessing hepatocellular carcinoma. Radiol Med. 2021;126:925–35.

[20] Laroia ST, Bhadoria AS, Venigalla Y, et al. Role of dual energy spectral computed tomography in characterization of hepatocellular carcinoma: initial experience from a tertiary liver care institute. Eur J Radiol Open. 2016;3:162–71.

[21] Ohira S, Kanayama N, Wada K, et al. Improvement of image quality and assessment of respiratory motion for hepatocellular carcinoma with portal vein tumor thrombosis using contrast-enhanced four-dimensional dual-energy computed tomography. PLoS One. 2021;16:e0244079.

[22] Secchi F, De Cecco CN, Spearman JV, et al. Monoenergetic extrapolation of cardiac dual energy CT for artifact reduction. Acta Radiologica. 2015;56:413–8.

[23] Kang HJ, Lee JM, Lee SM, et al. Value of virtual monochromatic spectral image of dual-layer spectral detector CT with noise reduction algorithm for image quality improvement in obese simulated body phantom. BMC Med Imaging. 2019;19:76.

[24] Popnoe DO, Ng CS, Zhou S, et al. Comparison of virtual to true unenhanced abdominal computed tomography images acquired using rapid kV-switching dual energy imaging. PLoS One. 2020;15:e0238582.

[25] Ascenti G, Mazziotti S, Mileto A, et al. Dual-source dual-energy CT evaluation of complex cystic renal masses. AJR Am J Roentgenol. 2012;199:1026–34.

[26] Dioguardi Burgio M, Sartoris R, Libotean C, et al. Lipiodol retention pattern after TACE for HCC is a predictor for local progression in lesions with complete response. Cancer Imag. 2019;19:75.

[27] Lee YJ, Lee JM, Lee JS, et al. Hepatocellular carcinoma: diagnostic performance of multidetector CT and MR imaging-a systematic review and meta-analysis. Radiology. 2015;275:97–109.

[28] Seo N, Kim MS, Park MS, et al. Evaluation of treatment response in hepatocellular carcinoma in the explanted liver with liver imaging reporting and data system version 2017. Eur Radiol. 2020;30:261–71.